Entanglement Detection with Quantum and Classical Kernels for SVMs

Ernesto Acosta[1,4 [0009−0001−4911−6819]], Carlos Cano[1,4 [0000−0002−0181−2444]], Daniel Manzano[2,4 [0000−0001−9241−5884]], and Guillermo Botella[3,4 [0000−0002−0848−2636]]

[1] Dept of Computer Science and AI, University of Granada, Spain
[2] Dept of Electromagnetism and Matter Physics, University of Granada, Spain
[3] Dept of Computer Architecture and Automation, Complutense University, Spain
[4] Quantum Thermodynamics and Computing Group, University of Granada, Spain

Abstract. The identification of quantum states separability remains a fundamental challenge in quantum information science [1, 2]. It is categorized as an NP-hard problem for dimensions exceeding 2×3, in which standard analytical tools like the Positive Partial Transpose (PPT) criterion are insufficient for detecting bound entangled states. This paper synthesizes our research on Quantum Support Vector Machines (QSVMs) employing both amplitude encoding [11] and Pauli feature map kernels [12]. We demonstrate that these models can effectively resolve complex state boundaries in 3×3, 4×4, and 5×5 systems, showing promising performance compared with classical kernel baselines.

Keywords: QSVM · QML · Entanglement · Quantum separability.

1 Introduction

Entanglement stands as one of the most profound and counterintuitive features of quantum mechanics, fundamentally distinguishing it from classical theories. It was considered by Schrödinger as the characteristic trait of quantum systems that enforces a departure from classical lines of thought [1]. Despite its pivotal role, the theoretical and practical characterization of entanglement remains an ongoing challenge [2].

Different Machine Learning (ML) approaches, notably Artificial Neural Networks [10], have been proposed for this task. More recently, Quantum Machine Learning (QML) tackles higher-dimensional spaces using models like Quantum Support Vector Machines (QSVMs). By replacing classical feature maps with quantum state encodings, QSVMs explore high-dimensional geometries that are potentially inaccessible to efficient classical computation.

This paper introduces the Quantum Separability Problem and reviews our group's work on QSVMs considering quantum-inspired kernels which are easy to simulate classically [11] and quantum kernels that are hard to simulate [12].

2 The Separability Problem

The state space of a quantum system is described by a complex Hilbert space $\mathcal{H}$ of dimension d. Quantum states can be classified as pure or mixed states [3,4]. In

this work, we focus on mixed states described by density operators $\rho \in \mathcal{B}(\mathcal{H})$[5], which are linear, positive semi-definite operators with unit trace ($\mathrm{Tr}[\rho] = 1$).

For a quantum system composed of two subsystems A and B (bipartite), the Hilbert space can be decomposed as $\mathcal{H} = \mathcal{H}_A \otimes \mathcal{H}_B$. A bipartite mixed state ρ is *separable* if it can be decomposed as a convex combination of product states:

$$\rho = \sum_j q_j \rho_{A,j} \otimes \rho_{B,j}, \qquad q_j \geq 0, \quad \sum_j q_j = 1. \tag{1}$$

with $\rho_{A,j} \in \mathcal{B}(\mathcal{H}_\mathcal{A})$ and $\rho_{B,j} \in \mathcal{B}(\mathcal{H}_\mathcal{B})$ $\forall j$. If no such decomposition exists, the state is *entangled* [2].

Determining if a state is separable is generally NP-hard for dimensions larger than 2×3 [5]. A standard tool for entanglement detection is the Peres-Horodecki Criterion [6,7], which is based on the Positive Partial Transpose (PPT) condition: a state $\rho \in \mathcal{B}(\mathcal{H}_A \otimes \mathcal{H}_B)$ has a Positive Partial Transpose (PPT) if its partial transpose is positive: $\rho^{T_B} \geq 0$. The Peres-Horodecki Theorem states that for dimensions 2×2 and 2×3, PPT is necessary and sufficient for separability. For higher dimensions (e.g., 3×3), PPT is necessary but not sufficient.

For the formulation of the quantum separability problem, we thus consider two different classes of mixed bipartite states (entangled and separable), and two subclasses of states for the entangled class (PPT Entangled and NPPT Entangled).

These categories are defined as: **Separable** states, which satisfy both Eq. (1) and the PPT condition; **PPT Entangled** states, which are entangled yet satisfy PPT; and **NPPT Entangled** states, which are entangled and violate PPT.

3 Quantum Support Vector Machines (QSVM)

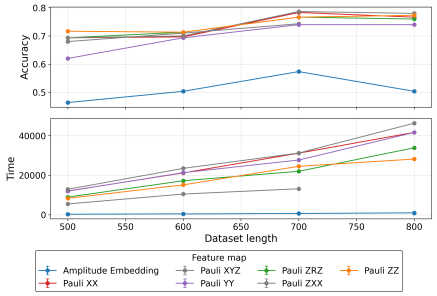
QSVMs extend classical SVMs by using quantum circuits as feature maps to compute similarity measures in high-dimensional Hilbert spaces [8].

Data Preparation Bipartite mixed states for 3×3, 4×4, and 5×5 systems were generated across three categories: (i) **Separable states**, constructed as product state convex combinations $\rho = \sum q_j \rho_{A,j} \otimes \rho_{B,j}$; (ii) **NPPT Entangled states**, generated by random sampling and filtered by PPT violation; and (iii) **PPT Entangled states**, identified via a Frank-Wolfe algorithm variant that retains PPT states exceeding a 0.01 distance threshold to their nearest separable approximation.

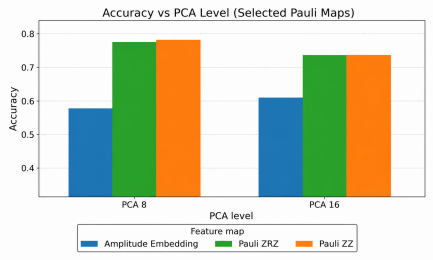
Dataset Partitioning: To target the complex separable–PPT boundary, the 2,000-sample training set uses only balanced separable and PPT entangled states (50% each). The test set evaluates all three categories equally. Test misclassifications show no NPPT concentration, confirming that training without NPPT states avoids bias against them.

Scaling: PCA compresses $d = 81$ vectors to 32–64 components (3×3 systems), enabling efficient quantum encoding while preserving entanglement traits.

[5] $\mathcal{B}(\mathcal{H})$ is the space of bounded operators acting on $\mathcal{H}$.



(a)Accuracy and time for different quantum kernels. Results for PCA = 8.



(b) Accuracy for PCA = 8 and PCA = 16, and dataset length = 700.

Fig. 1: Comparison of performance for different kernel settings. Time is measured in ms and includes both kernel generation and SVM training.

3.1 Amplitude Embedding Kernel

Amplitude encoding maps a classical vector x into $|\psi_x\rangle = \frac{1}{\|x\|_2}\sum_{i=0}^{N-1} x_i|i\rangle$, yielding the kernel $K(x,y) = |\langle\psi_x|\psi_y\rangle|^2$. This corresponds to a normalized homogeneous polynomial kernel of degree two.

3.2 Pauli Feature Map Kernel

To leverage classically hard-to-simulate quantum circuits, we employ Pauli feature maps [9] $U_\phi(x) = \exp\big(i\sum_{S\subseteq\{1,\ldots,n\}}\phi_S(x)\prod_{j\in S}P_j\big)$, with Pauli strings $P_j \in \{X_j, Y_j, Z_j\}$ and data coefficients $\phi_S(x)$. The resulting kernel $K_\phi(x,y) = \big|\langle 0^{\otimes n}|U_\phi^\dagger(x)U_\phi(y)|0^{\otimes n}\rangle\big|^2$ measures quantum state overlap across tested ZZ, ZRZ, and ZXX architectures [12].

4 Experiments and conclusions

We performed experiments involving 3×3, 4×4, and 5×5 systems. This section summarizes some of the most relevant results and main takeaways from [11, 12].

Amplitude embedding kernel. Amplitude embedding kernels reached accuracies of up to 80% for 3×3, 90% for 4×4, and nearly 100% for 5×5 systems. The use of Principal Component Analysis (PCA) was revealed essential for bridging high-dimensional data with limited qubits. For 3×3 systems, 64 components provided the best results among tested configurations in this case [11].

Pauli feature map kernel. In [12] we performed a targeted study on 3×3 systems comparing amplitude encoding with Pauli feature maps. Figure 1 shows some of the results of this comparison.

At PCA=8, the Pauli-ZZ kernel achieves 78% accuracy versus 57% for amplitude encoding, demonstrating greater resistance to information loss during dimensionality reduction. Overall, Pauli-ZZ and ZRZ kernels require significantly fewer features (8 vs. 32) for comparable accuracy due to superior expressivity in

low-dimensional spaces. Although classically expensive to simulate, Pauli feature maps remain promising candidates for quantum hardware speedups. Ultimately, these findings reveal a trade-off between classical simulability and quantum expressivity: amplitude encoding is effective for high-dimensional (5×5) systems with scaled PCA, while Pauli feature maps dominate low-dimensional regimes.

Acknowledgments. This publication is part of the R+D projects PID2024-162155OB-I00, PID2024-162141OB-I00 and PID2024-158203OB-I00 funded by MICIU/AEI/10.13039/501100011033/ERDF/EU, as well as the Ministry of Economic Affairs and Digital Transformation of the Spanish Government through the QUANTUM ENIA project call - Quantum Spain project. Also grant C-EXP-251-UGR23 funded by Consejería de Universidad, Investigación e Innovación and by ERDF Andalusia Program 2021-2027. Finally, we are grateful for the technical support provided by PROTEUS, the supercomputing center of the Institute Carlos I for Theoretical and Computational Physics in Granada, Spain.

Disclosure of Interests. The authors have no competing interests to declare that are relevant to the content of this article.

References

1. E. Schrödinger,"Discussion of probability relations between separated systems", *Proceedings of the Cambridge Philosophical Society* **31**, 555–563 (1935).
2. R. Horodecki, P. Horodecki, M. Horodecki, and K. Horodecki, "Quantum entanglement", *Rev. Mod. Phys.* **81**, 865–942 (2009).
3. A. Galindo and P. Pascual, *Quantum Mechanics I & II*, Springer-Verlag, Berlin, 1990
4. M. A. Nielsen and I. L. Chuang, *Quantum Computation and Quantum Information*, 10th Anniversary Edition, Cambridge University Press, Cambridge, 2010.
5. O. Gühne and G. Tóth, *Entanglement detection*, Phys. Rep. **474**, 1–75 (2009).
6. A. Peres, *Separability Criterion for Density Matrices*, Phys. Rev. Lett. **77**, 1413–1415 (1996).
7. M. Horodecki, P. Horodecki, and R. Horodecki, *Separability of mixed states: necessary and sufficient conditions*, Phys. Lett. A **223**, 1–8 (1996).
8. M. Schuld and N. Killoran, "Quantum machine learning in feature Hilbert spaces", *Physical Review Letters*, vol. 122, no. 4, Art. no. 040504, 2019.
9. V. Havlíček, A. D. Córcoles, K. Temme, A. W. Harrow, A. Kandala, J. M. Chow, and J. M. Gambetta, "Supervised learning with quantum-enhanced feature spaces", *Nature*, vol. 567, pp. 209–212, 2019.
10. J. Ureña, A. Sojo, J. Bermejo-Vega, D. Manzano, "Entanglement detection with classical deep neural networks", *Scientific Reports*, vol. 14, Art. no. 18109, 2024.
11. A. Martínez-Sabiote, M. Skotiniotis, J. J. Bermejo-Vega, D. Manzano, and C. Cano, "Entanglement Detection with Quantum-inspired Kernels and SVMs", *The Journal of Supercomputing*, col. 82, Art. no 100, (2026)
12. E. Acosta, C. Cano, D. Manzano, and G. Botella, "Quantum Kernels for SVM Entanglement Detection", in *Proc. IEEE Conference on Artificial Intelligence 2026 (CAI)*, Granada, Spain, 2026.